JADVE

Journal of Advances in Vehicle Engineering 5(1) (2018) 10-17
www.jadve.com

Development of a numerical model of railway air brake and validation against experimental data

Stefano Melzi*[1], Angelo Grasso[2]

[1]*Politecnico di Milano,Department of Mechanical Engineering,via La Masa 1, 20156, Milan (MI), Italy*

[2]*Faiveley Transport (Wabtec Company)*

** stefano.melzi@polimi.it*

(Manuscript Received: 18 June 2018; Revised: 23 October 2018; Accepted: 11 November 2018)

Abstract

The paper presents a model for the pneumatic part of UIC air brake, aiming at the prediction of the dynamics of compressed air in main braking pipe and braking cylinders. A lumped parameter scheme, based on an equivalent electrical circuit, is used to model the main braking pipe; the proposed scheme allows venting the pipe from different positions. Pressure build-up in braking cylinders is determined by the dynamics of pressure drop in main braking pipe and by the crossing of pressure thresholds. Time histories of pressure drop in main braking pipe and pressure build-up in braking cylinders were compared with experimental data collected with an indoor test facility to tune some of the model parameters and to validate the model itself.

***Keywords*:** railway air brake, main braking pipe, brake cylinder, numerical model, numerical-experimental comparison.

1. Introduction

UIC air brake is based on a design originally developed by George Westinghouse in the second half of the XIX century. This braking system is characterized by a main braking pipe (MBP) which runs along the entire train: each wagon contains in fact a segment of the pipe; when wagons are linked together, extremities of the pipe are also joined so that a continuous system is obtained. Compressors in locomotives can raise the pressure in MBP up to a reference value (5 bar for trains operating in Europe); in this state reservoirs in each wagon are filled with compressed air and brakes are released. When braking is commanded, pressure in main braking pipe is decreased by connecting it to the atmosphere. Venting the MBP pipe opens valves between reservoirs and braking cylinders; these lasts are then filled with compressed air and can apply a force to the braking pads. Braking command is thus conveyed along the train via propagation of a pressure drop wave in the MBP. In case of train disruption, the subsequent pressure loss in MBP causes the brakes to activate and the train to stop.

The effect of braking system on stopping distances is obvious but the same system has an important impact also on the coupling forces among wagons. As the braking signal is conveyed through the propagation of a pressure wave, brakes activate earlier in the first part of the train (i.e. where the braking command starts in normal operating conditions), while their intervention is delayed in the rear part. As a consequence, the rear part of the train tends to bump against the front one causing a rise of compression forces in buffers. This effect is particularly important for very long freight trains where the delay joined with the mass of the wagons significantly excites the longitudinal dynamics of the whole train: compression/dilation waves may arise, causing large compression and tension forces in couplers [1][2]. Excessive tension forces may result in train disruption, while excessive compression forces may have serious consequences on running safety [3].

The work presented in the paper was carried out as part of DYNAFREIGHT project (Innovative technical solutions for improved train DYNAmics and operation of longer FREIGHt Trains), a European research project within the Horizon 2020 programme of the European Commission [4]. The final goal of the project is to provide the necessary inputs for the development of the next railway freight propulsion concepts within Shift2Rail Innovation Programme 5. More in detail, part of the project is focused on the possibility of increasing the length of European freight trains up to 1500 m, using several locomotives distributed along the train-set synchronized via radio inputs. Numerical simulations were carried out to assess the safety of these long freight trains considering a series of parameters like coupling forces and stopping distances in critical scenarios. The activity presented in this paper concerns the modelling of the pneumatic part of the UIC braking system; in particular the model aims at predicting the dynamics of the compressed air in the MBP and the pressure build-up in braking cylinders. In DYNAFREIGHT, data generated with the pneumatic-brake model were then used as input by other partners to simulate the dynamics of the whole train-set through multi-body models.

The paper is organized as follows: as first, a brief description of the components of the pneumatic brake is provided. The numerical model of the pneumatic brake is then described

in details. The last section deals with the comparisons between numerical and experimental results.

2. The UIC air brake

An exhaustive explanation of the functioning of UIC air brake can be found in [5] and [6]. The main components are hereafter briefly described.

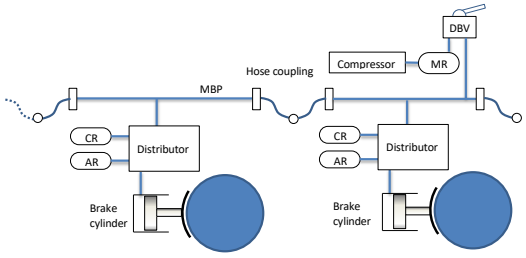

Figure 1. Main components of air brake system and connection between adjacent vehicles.

Referring to Figure 1, the pressure inside MBP is controlled through the driver braking valve (DBV). Acting on the DBV, the driver can fill the MBP with compressed air coming from the compressor or the main reservoir (MR); once a reference value is reached (5 bar), air inside command reservoirs (CR) and auxiliary reservoirs (AR) is at 5 bars too, while pressure in brake cylinders is at 0 bar. In this condition, brakes are released.

To perform a service braking, the driver can control the pressure at DBV extremity, setting a reference value approximately between 3 and 4.5 bar. When emergency braking is demanded, the driver connects the MBP directly with the atmosphere through a large opening. Both the commands cause the pressure in MBP to decrease, the emergency braking producing a faster and larger pressure drop. As the distributor detects a difference between pressures of CR and MBP lager than 0.3 bar, the AR is connected to the BC; consequently, the pressure inside cylinders rises up to a level proportional to the pressure difference between MBP and CR. When this happens, the connection between BC and AR is closed and pressure is maintained inside the cylinder. Further pressure drops in MBP will lead to higher pressures in BC; the maximum braking pressure is reached when a pressure difference of 1.5 bar (or higher) is established between CR and MBP.

During braking release, the charging of MBP from the loco causes the BC to be connected to the atmosphere. Again, the difference of pressure between CR and MBP drives the opening of the connection between BC and atmosphere. In other words, the braking intensity can be controlled also during the braking release phase by controlling the value of pressure in MBP.

Distributors are quite complex elements which include several components influencing the pressure build-up process in braking cylinders: the accelerating chamber, the first-phase device, the freight-passenger device.

The accelerating chamber is a volume of air at atmospheric pressure which is automatically connected to the MBP during the first instants of the braking. In this way the compressed air in MBP is released towards the chamber speeding up the venting process. Due to its small volume, the accelerating chamber is able to produce just a sudden drop of pressure in MBP (between 0.3-0.4 bar) at the beginning of the venting. Once the accelerating chamber is filled with compressed air, it is excluded from the pneumatic circuit until brakes are released.

The first-phase device provides a large-opening connection between AR and BC during the first instants of the braking. This device allows the braking cylinder to be rapidly filled with compressed air and to apply nearly 15% its maximum force almost at once. As the cylinder is getting filled, the large opening of the first-phase device is gradually closed and the filling process is completed through a smaller calibrated orifice.

The freight-passenger device was developed because freight trains are usually longer and heavier than passenger ones. Considering the delay in propagation of braking command from the train head to its tail discussed in the introduction, freight trains are in general subjected to higher coupling forces which can undermine both their safety and integrity. For this reasons the so-called ”G braking regime” (where G refers to “Goods”) is adopted for long freight trains: with this operating condition, the pressure build-up in cylinders in completed between 18-30 s. When “P braking regime” is used (where P refers to “Passenger”), the pressure build-up is instead completed between 3-7 s. The freight-passenger device thus changes the section of the calibrated orifice connecting the AR with the cylinder resulting in different filling times. The longer time required to complete the pressure build-up results in lower solicitations on the coupling elements.

The schematic of Figure 1 assumes the presence of one single DBV at the train head; actually, especially when operating long freights, several traction units may be used, each one provided with a DBV. This means that MBP can be vented from different points simultaneously or with small delays. it is indeed possible that, due to errors, conflicting commands are applied causing the MBP to be vented by one DBV and filled by another one.

When dealing with long freight trains, the dynamics of the air brake and the aspects discussed before should be properly modelled in order to make realistic predictions of both stopping distances and coupling forces.

3. Modelling of the UIC Brake

Different models of the pneumatic brake system were presented in technical literature since the late 50’s [7]; in recent years several model were proposed with different degrees of detail and complexity. In [8] the dynamics of the compressed air in main braking pipe is described through an analytical formulation assuming a one-dimensional isothermal flow moving in a circular pipe. Resulting partial differential equations are then implemented and solved through a finite ele-

ment formulation. A detailed model of an automatic brake valve is also included. The authors of [6] proposed a tool for the modelling of the UIC air-brake allowing assembling segments of pipes, reservoirs, and more complex components like distributors or brake cylinders. A general scheme can be then implemented and solved in MATLAB environment. A constant-area, isothermal and one-dimensional flow is again assumed for the MBP model; the distributor model is made up of several chambers connected through valves whose opening is regulated by a state-flow chart able to reproduce the logic of the device. In [5] the MBP is modelled as a circular pipe with variable diameter to include the effect of couplings between adjacent vehicles. An analytical model of a one-dimensional flow is again used but this time also the specific energy of the fluid is introduced as state variable to remove the hypothesis of isothermal flow. A simplified model for the filling process of braking cylinders is used. In [9] a model similar to [5] is used for the MBP: the airflow is assumed one-dimensional and non-homoentropic and a complex model for the distributor is used. All the models appear able to correctly match time histories of pressure in MBP and in BCs measured on the corresponding real devices.

The model presented in this paper is basically an evolution of the one presented in [3]. The main difference with respect to the other models described in technical literature, is the schematisation of the main braking pipe which is based on a lumped parameter model. The model is thus simpler and its computation faster. Models of the distributors similar to those of [5] are also used. Despite the adopted simplifications, the model allows to accurately reproduce the dynamics of compressed air in main braking pipe and braking cylinders during braking manoeuvres.

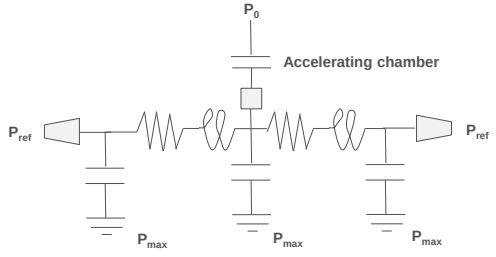

Figure 2. lumped parameter model of main braking pipe for 1 vehicle

4. Main braking pipe model

The brake model developed in this research describes the dynamic of compressed air inside MBP through a lumped parameter scheme; the MBP is divided into several sections, each one characterized by an equivalent electric scheme. According to this model, fluid internal friction is reproduced with resistance elements, inertial effects are represented through inductance elements and fluid compressibility is modelled with capacitance elements. Figure 2 shows the scheme used to discretize the main braking pipe on the single vehicle.

As depicted in Figure 2, the MBP of a single vehicle is divided into two sections. A boundary condition P_{ref} is imposed at the pipe extremities to simulate venting or refilling of the pipe itself through two valves. P_{max} represents the nominal pressure inside MBP when braking is not applied (5 bar) and P_0 is the atmospheric pressure (0 bar). Each vehicle is also characterized with an accelerating chamber, an element of the brake distributor, which is supposed to be at the centre of the vehicle. The accelerating chamber is modelled as a volume at atmospheric pressure connected to the MBP through a valve whose opening is regulated by the pressure drop in MBP.

When several vehicles are joined together, the model of the MBP is simply derived by connecting in series several models of the kind of Figure 2. As shown in Figure 3, the pipe is provided with valves at the extremities of each single vehicle: this allows simulating venting of MBP from different points along the train. $P_{ref,I}$ represents a boundary condition, in general function of time; the difference between $P_{ref,I}$ and the pressure of the pipe in the corresponding section determines the flow crossing the i-*th* valve.

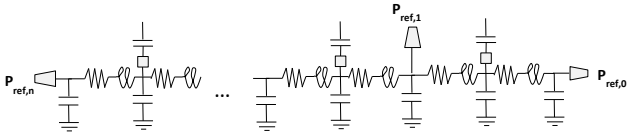

Figure 3. Model of the entire main braking pipe

If an emergency braking is commanded from the 1st vehicle, $P_{ref,0}$ will be set to 0 bar while the generic $P_{ref,I}$ will take the value of the corresponding pressure inside the pipe (that is: no air flow will cross the other valves). When a maximum service braking is performed from the 1st vehicle, $P_{ref,0}$ will be set to 3 bar. Sections of the venting valve change according to the type of braking: a larger section is used when emergency braking is performed. The presence of multiple valves along the pipe allows for example to perform an emergency braking from the train head and a simultaneous maximum service braking commanded by a second loco in a different position along the convoy.

As aforementioned, resistance of the equivalent electric circuit is representative for the internal friction of fluid. The resistance of a section of the main braking pipe was estimated according to the model proposed in [7]. In particular, the pressure drop across a segment of pipe of length *l* is given by:

$$\Delta p = \lambda \rho \frac{w^2}{2} \frac{l}{D} \tag{1}$$

Where λ is the dimensionless friction coefficient; w is the fluid average speed (1D flow); ρ is the fluid density; D is the pipe diameter.

The fluid average speed is related to the mass flow *G* by:

$$G = \rho \frac{\pi D^2}{4} \cdot w \tag{2}$$

The fluid speed is thus given by:

$$w = \frac{1}{\rho}\frac{4G}{\pi D} \tag{3}$$

Combining equation (1) with equation (3), the pressure drop across the section of main braking pipe can thus be expressed as function of the mass flow as:

$$\Delta p = \lambda \frac{\rho l}{2D}\frac{16}{\rho^2\pi^2 D^4}G^2 = \lambda \frac{8l}{\rho\pi^2 D^5}G^2 \tag{4}$$

The dimensionless friction coefficient λ is function of the Reynolds number Re:

$$\mathrm{Re} = \frac{4G}{\pi D\mu} \tag{5}$$

Air viscosity μ is estimated using the empirical relationship:

$$\mu = \left(1.84 - \frac{300 - T}{300}\right)\cdot 10^{-5} \tag{6}$$

Where T is the fluid temperature in K. Dependence of λ from Re can be expressed through the following formula [7]:

$$\lambda = \frac{1}{\left(2\log\left(0.5625\,\mathrm{Re}^{\frac{7}{8}}\right) - 0.8\right)} \tag{7}$$

The pressure drop across a section of pipe is thus function of the fluid density and the mass flow-rate:

$$\Delta p = R(\rho, G) \tag{8}$$

where $R(\rho,G)$ represents the fluid resistance. The value of l used to compute resistance takes into account the length of the vehicle, adding up the length of connections between adjacent vehicles and increasing the value by 7.5% to consider additional resistances due to curves and concentrated pressure losses. The fluid density ρ is function of the density ρ_N measured in standard conditions (ANR).

$$\rho = \rho_N \frac{P}{P_N}\frac{T_N}{T} \tag{9}$$

T_N and P_N respectively represent the temperature and pressure in standard conditions. While integrating the equations of main braking pipe, value of resistance is thus updated at each integration step to consider variation of density. Temperature inside MBP is evaluated from its pressure under the hypothesis of adiabatic flow.

Inductances are used to represent the inertial effects of compressed air. The value of inductance L is simply given by:

$$L = \frac{4l}{\pi D^2} \tag{10}$$

The capacitance is introduced to model the fluid elasticity. The overall capacitance of a vehicle is obtained as:

$$C = \frac{\pi D^2 l}{4}\frac{1}{\hat{R}T} \tag{11}$$

where $\hat{R}$ is the universal gas constant and T is the temperature; again, the values of capacitances are updated at each integration step as local temperature changes with pressure. The capacitance of the vehicle is distributed over three capacitances (Figure 2); in particular 50% of the total capacitance is assigned to the central capacitor. The remaining 50% is equally divided between the capacitor at vehicle's extremities. Simulation of venting of main braking pipe is performed creating a connection between the pipe and one or more volumes at a reference pressure $p_{ref,i}$ opening corresponding nozzles along the pipe. The area of the nozzles depends on the braking manoeuvre type, i.e. larger for an emergency braking and smaller for a service braking. Transition of flux from sonic to subsonic is considered when venting the main braking pipe as well as when accelerating chambers activate. Accelerating chambers are modelled as volumes whose value is one of the model inputs; the nominal pressure of accelerating chambers is equal to the atmospheric one (P_0) when braking is not activated. As braking is commanded and pressure inside MBP drops, nozzles between main braking pipe and accelerating chambers open automatically and air flows inside their volumes. The flux is unidirectional and stops when pressure inside accelerating chamber is equal to the pressure in the MBP.

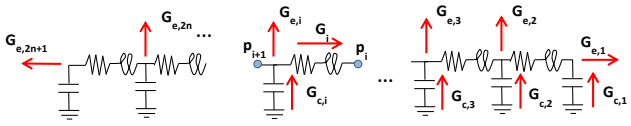

Figure 4. Flows and pressures at nodal points in the lumped parameter model of MBP.

The equivalent electric scheme of Figure 4 is characterised by 2n unknowns corresponding to the internal flows in the brake pipe segments plus other 2n+1 unknowns representing the pressures at nodal points. It is possible to write 2n equations for the pressure drop across the i-th segment of braking pipe:

$$p_{i+1} - p_i = R_i G_i + L_i \dot{G}_i \tag{12}$$

Where G_i is the airflow in the i-th segment of the pipe. G_i can be computed as:

$$G_i + \sum_{k=1}^{i} G_{ck} = \sum_{k=1}^{i} G_{ek} \tag{13}$$

In equation (13), G_{ek} and G_{ck} are respectively the flows leaving and entering the pipe in the k-th nodal point. G_{ek} is associated with the flow directed towards accelerating chambers or venting nozzles and it is a non-linear function of p_k. G_{ck} is instead related to the flow provided by the air already contained in the braking pipe and can be expressed as:

$$G_{ck} = -C_k \dot{p}_k \tag{14}$$

Equation (14) can thus be rewritten as:

$$G_i + \sum_{k=1}^{i} -C_k \dot{p}_k = \sum_{k=1}^{i} G_{ek} \tag{1}$$

Besides the 2n equations of this kind, it is possible to add another equation for the total flow, which includes also the flow leaving the pipe from the train end:

$$\sum_{k=1}^{2n+1} G_{ck} = \sum_{k=1}^{2n+1} G_{ek} \tag{15}$$

Altogether, equations (12),(15) and (16) represent a set of 4n+1 non-linear 1-st order differential equations. The system state is identified through the vector X defined as:

$$\mathbf{x} = \{p_1 \quad p_2 \quad \dots \quad p_{2n+1} \quad G_1 \quad G_2 \quad \dots \quad G_{2n}\}^T \tag{16}$$

The problem can be therefore formulated as:

$$[\mathbf{A}(\mathbf{x})]\dot{\mathbf{x}} = \mathbf{Q}(\mathbf{x}) \tag{17}$$

Solving the system of differential equations allows to determine the time histories of flows and, more important, of pressure inside different sections of the MBP.

5. Brake distributor model

The model for the brake distributor takes as input the pressure drop in the main braking pipe in the range 0.3-1.5 bar. With a pressure drop of 1.5 bar, the braking cylinder develops the maximum braking force. Figure 5a shows a time history of pressure in main braking pipe; Figure 5b displays the corresponding pressure drop with saturation at 1.5 bar.

The signal reported in Figure 5b represents the "command" signal for the brake cylinder. This signal is processed considering the crossing of thresholds associated with the intervention of the first-phase device, which speeds-up the filling of cylinders in the first part of the braking (Figure 6). Once the first-phase device intervention ends, the pressure build-up follows the gradient associated with the braking regime (P or G) up to a value determined by the pressure drop in main braking pipe. With a pressure drop of 1.5 bar, the air in the cylinder reaches the maximum value and the cylinder will develop the maximum braking force.

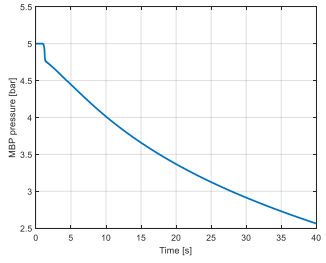

a

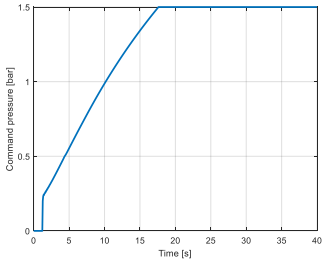

b

Figure 5. Pressure drop in main braking pipe (a); corresponding pressure command signal to brake cylinder

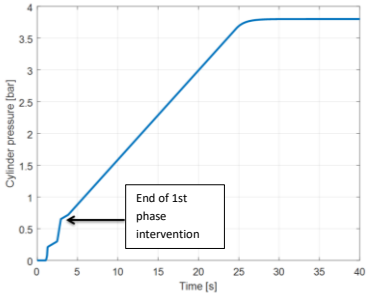

Figure 6. Pressure build-up in brake cylinder.

6. Numerical-experimental comparison

The models developed to describe the dynamics of compressed air in main braking pipe and in braking cylinders were tested against experimental data. Experimental tests were carried out by "Favelay Transport" using an indoor test facility specifically developed to characterize the response of the UIC brake. In particular, the test facility is made up of segments of steel tubes of the same diameter of the pipe of freight trains (i.e. 5/4 inches) connected in series to reproduce the configuration of a MBP on a real train. DBV valves are introduced in several positions of the pneumatic circuit to allow venting the main braking pipe from different positions. Pressure sensors were used to record the time history of pressure in MBP and in brake cylinders in several points along the pipe.

During experimental tests a series of emergency braking and maximum service braking manoeuvres were performed considering both P and G regimes with train lengths up to 1500 m.

Experimental data were used to tune some parameters of the model like the fluid internal resistance and sections of the nozzles for emergency braking and maximum service braking. More in detail, comparisons between experimental and numerical results revealed that the correct value of fluid resistance in MBP could be obtained considering an effective diameter of the pipe equal to 70% the real value. The efflux area for service braking is about 15% the one used for emergency braking.

Several experiments were carried out considering braking manoeuvres commanded by a loco in the train head. Both emergency braking and maximum service braking were considered for trains with lengths between 400m and 1200 m. In addition, venting MBP from two different points was reproduced with the test bench for a 1500m-long train.

7. Emergency braking

Eight emergency braking manoeuvres were performed with the test bench considering trains of four different lengths: 400m, 750, 1000m and 1200 m. Both braking regimes P and G were tested. Pressure in MBP and braking cylinders were recorded in 10 positions along the pneumatic circuit.

Figure 7a reports a comparison between numerical and experimental results relevant to the time histories of pressure drop in MBP and of pressure build-up in braking cylinder for

the first and last vehicle. The test refers to a 750m-long train performing an emergency brake in regime P. The match between experimental and numerical results can be considered satisfactory. Figure 7b shows the time required to reach a given pressure in MBP or in braking cylinders in different positions along the train. In particular, the red line identifies the position and the time instant corresponding to a pressure drop of 0.3 bar in the MBP; this value allows opening the connection between the auxiliary reservoir and the brake cylinder. The red line thus indicates the beginning of pressure build-up in brake cylinders. The blue line corresponds to a pressure drop of 1.5 bar in MBP; any further drop does not have any influence over the pressure achieved in brake cylinder. The black line shows when and where the braking cylinders are developing 90% of their maximum force. Results of Figure 7b are obtained exploiting the complete measuring set-up and indicate that the proposed model is able to correctly predict the dynamics of pressure in MBP and brake cylinders in several positions along the train.

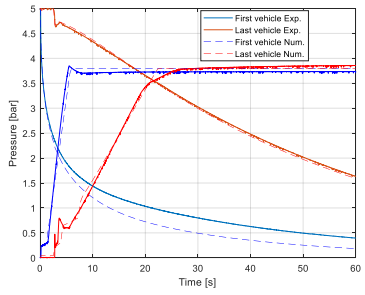

a

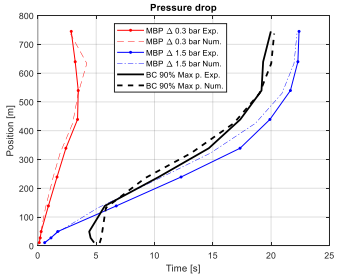

b

Figure 7. 750m-long train, emergency braking in regime P; (a): time histories of pressure drop in main braking pipe and pressure build-up in braking cylinders for the first and last vehicles; (b) time required for reaching given pressure drops in MBP and to reach 90% of the maximum force in braking cylinders.

Figure 8 displays the results referred to all the emergency braking manoeuvres. Figure 8a compares the time required to complete a pressure drop of 1.5 bar in MBP in the last vehicle; looking at the labels of the chart, "E" indicates "Emergency" braking, while G and P are relevant to the braking regime. The performance of the MBP model can be evaluated through the data of Figure 8a: the times predicted by the model are very close to those measured during the tests. This result was achieved tuning one of the model parameters, i.e. the equivalent diameter of the MBP. Considering Eq. (4), the diameter used in simulation was 70% the nominal one. It is possible to notice that times required to produce a pressure drop of 1.5 bar in MBP are almost the same with P or G regime as this last just affects the filling time of brake cylinders. The bars of Figure 8b compare the times required to reach 90% of the maximum force in the brake cylinder of the last vehicle. In this case, the effect of braking regime is clearly visible. Results are again good, showing that also the dynamic of pressure build-up in braking cylinder is correctly reproduced by the model. Looking at Figure 8b reveals how braking regime becomes in fact ineffective for trains longer than 1000m; in this case, the time required to vent the MBP is much more important than the delay in filling the braking cylinders associated with the braking regime.

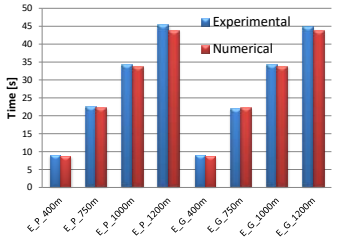

a

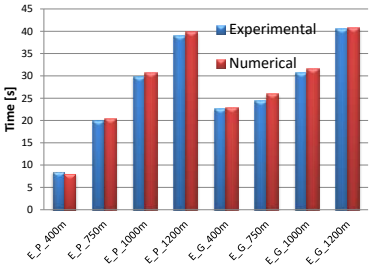

b

Figure 8. Emergency braking in P and G regimes. (a): time required to produce a pressure drop of 1.5 bar in MBP in the last vehicle; (b) time required to reach 90% of the maximum force in braking cylinder of the last vehicle.

8. Maximum service braking

A second series of tests was carried out performing maximum service braking manoeuvres. Again, 4 trains of different lengths were considered: 400 m, 750m, 1000m and 1200m. These manoeuvres allowed to tune the section of the valve for venting the MBP during a maximum service braking; its area resulted approximately 15% the one used to match the data of an emergency braking.

The picture of Figure 9a shows the pressure drop in MBP and the pressure build-up in brake cylinder for the first and last vehicle of a 1000m-long train. The transient appears significantly longer with respect to the data of Figure 7 due to several reasons: longer train, braking regime G and reference pressure at DBV around to 3.25 bar against 0 bar used for an emergency braking. In addition, in this case the comparison between experimental and numerical results can be considered satisfying.

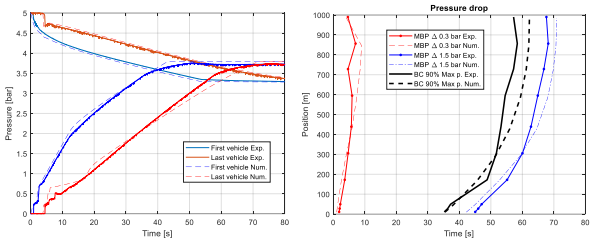

Figure 9. 1000m-long train, maximum service braking in regime G; (a): time histories of pressure drop in main braking pipe and pressure build-up in braking cylinders for first and last vehicles; (b) time required for reaching given pressure drops in MBP and to reach 90% of the maximum pressure in braking cylinders

Figure 9b reports the time instants when meaningful values of pressure are reached in MBP or brake cylinders for different positions along the train. These results confirm that the model is suitable for reproducing the dynamics of compressed air in MBP: maximum differences are below 4s (over 60s). As far as the pressure build-up in brake cylinders is concerned, results can be considered reasonably good, with a maximum difference of nearly 6 seconds (over 60s) when estimating the time required to reach 90% of the maximum force.

Figure 10 reports eight comparisons between numerical and experimental results referred to the last vehicle of the trains. The bars of Figure 10a indicate the time required to complete a pressure drop of 1.5 bar in the MBP; results are good for trains up to 1000 m, while a difference of about 5 s is revealed for the longer train. However, the relative error in this case is about 6%, which appears reasonable. Comparing the times required to reach 90% of the maximum force puts into evidence more discrepancies with respect to the emergency braking case. Figure 10b reveals a very good agreement for trains up to 750m; when longer trains are considered, differences up to 7s (over 70s) are obtained.

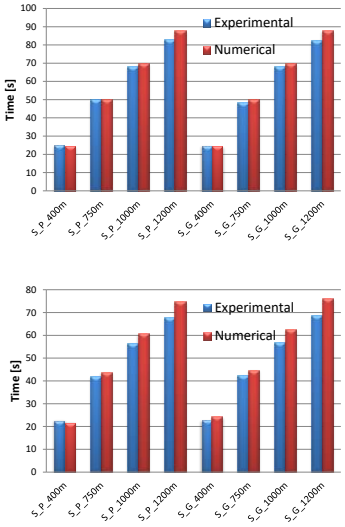

Figure 10. Emergency braking in P and G regimes. (a): time required to produce a pressure drop of 1.5 bar in MBP in the last vehicle; (b) time required to reach 90% the maximum force in braking cylinder of the last vehicle.

9. Venting MBP from different positions

As last scenario, venting main braking pipe from different positions at the same time was taken into account. In this scenario, the pipe of 1500-m long train was reproduced in the indoor test facility and equipped with 2 DBVs: one at the train head and another at the train centre. Pressures in MBP and in brake cylinders were measured in 7 points along the train. In this manoeuvre, the head loco commands a maximum service braking form the train head; the slave loco reproduces the same command with a delay of 3s.

Figure 11a shows the time histories of pressure drop in MBP and pressure build-up in brake cylinders for the first and last vehicles. The model correctly reproduces the transient of pressure drop in MBP. Pressure build-up for the first vehicle is in good agreement with experimental. Few discrepancies instead appear for the last vehicle, even if the filling time of the cylinder is correct.

Considering now the comparison of meaningful values of pressure thresholds in MBP and brake cylinder, Figure 11b reveals the good performance of the model of the MBP. Also the prediction of the time required to reach 90% of the maximum force in cylinders appears quite good: the maximum error is approximately 5s over 50s.

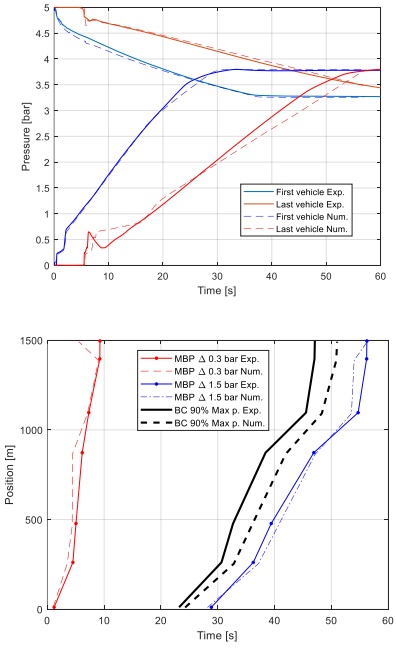

Figure 11. 1500m-long train, maximum service braking in regime G venting pipe from train head and train centre; (a): time histories of pressure drop in main braking pipe and pressure build-up in braking cylinders for first and last vehicles; (b) time required for reaching given pressure drops in MBP and to reach 90% of the maximum force in braking cylinders.

Conclusions

A mathematical model for UIC air brake was presented: the model simulates the venting of MBP and the pressure build-up in brake cylinders. The core of the model is a lumped parameter model of the MBP, which is described through an equivalent electric scheme where resistances, capacitances and inductances respectively represent the internal dissipation, the elasticity and the inertia of the compressed air. The model allows to reproduce venting of MBP from several positions along its length and includes models for different components of brake distributors like: accelerating chambers, first-phase devices, freight-passenger devices.

Experimental data obtained thanks to a test facility and provided by Favelay Transport, allowed to tune some of the model parameters. At present state, the model appears capable of reproducing with reasonable accuracy the dynamics of compressed air in MBP and the process of pressure build-up in brake cylinders. **Table 1** reports the relative errors in the estimates of the time needed to cross meaningful thresholds of pressure in MBP and brake cylinders for the last vehicle of the various trains considered. Maximum errors are below 6.2% for the MBP and slightly above 10% for brake cylinders.

Table 1. Relative errors referred to the last vehicle; 1st column: time required to produce a drop of 1.5 bar in the MBP; 2nd column: time required to develop 90% of the maximum force in the brake cylinder.

Train	MBP: 1.5 bar drop	Cylinder: 90% Fmax
E_P_400m	-4,49%	-5,72%
E_P_750m	-0,80%	1,45%
E_P_1000m	-1,08%	2,88%
E_P_1200m	-3,42%	1,87%
E_G_400m	-4,07%	1,20%
E_G_750m	1,55%	6,11%
E_G_1000m	-1,14%	2,67%
E_G_1200m	-2,56%	0,44%
S_P_400m	-1,48%	-4,14%
S_P_750m	0,60%	4,25%
S_P_1000m	2,62%	7,66%
S_P_1200m	5,90%	10,01%
S_G_400m	-0,88%	6,45%
S_G_750m	4,22%	5,02%
S_G_1000m	2,44%	9,81%
S_G_1200m	6,18%	10,53%
S_G_1500m (venting from 2 positions)	0,32%	10,38%

Acknowledgements

Authors would like to thank Shift2Rail Innovation Programme 5 and the partners of Dynafreight project.

References

[1] Cole C, McClanachan M, Spiryagin M, et al. Wagon instability in long trains. Vehicle System Dynamics 2012; 50 (Suppl. 1) 303–317. https://doi.org/10.1080/00423114.2012.659742

[2] Zhang Z, Li G, Chu G, et al. Compressed stability analysis of the coupler and buffer system of heavy-haul locomotives. Vehicle System Dynamics 2015; 53(6), 833–855;https://doi.org/10.1080/00423114.2015.1023318

[3] Belforte P., Cheli F., Diana G.,Melzi S.,Numerical and experimental approach for the evaluation of severe longitudinal dynamics of heavy freight trains, Vehicle System Dynamics Vol. 46, Supplement, 2008, 937–955;https://doi.org/10.1080/00423110802037180

[4] Vaghi, C., Berg, M., Long freight trains in Europe: Assessing the requirements and safety issues, Global Railway Review, Volume 24, Issue 01, 5-9, 2018

[5] Cantone L., TrainDy: the new Union Internationale des Chemins de Fer software for freight train interoperability, Proc. IMechE Vol. 225 Part F: J. Rail and Rapid Transit, 57-70, 2009;https://doi.org/10.1243/09544097JRRT347

[6] Pugi L., Malvezzi M., Allotta B., Banchi L. and Presciani P., A parametric library for the simulation of a Union Internationale des Chemins de Fer (UIC), Proc. Instn Mech. Engrs Vol. 218 Part F: J. Rail and Rapid Transit, 117-132, 2004; https://doi.org/10.1243/0954409041319632

[7] Carello M., Ivanov A., Mazza A., Pressure drop in pipe lines for compressed air: comparison between experimental and theoretical analysis, transactions on Engineering Sciences vol 18, 1998, WIT Press, ISSN 1743-3533.

[8] Specchia A., Afshari, Shabana A Ahmed, Caldwell N., A train air brake force model: Locomotive automatic brake valve and brake pipe flow formulation. Journal of Rail and Rapid Transit, 227 (1) 19-37. DOI: 10.1177/0954409712447230

[9] Wei W., Yang H.,Qing W.,Xubao Z., Zhang J., Zhang Y. An air brake model for longitudinal train dynamics studies, Vehicle System Dynamics, 55:4, 517-533, DOI: 10.1080/00423114.2016.1254261

[10] Carello M., Ivanov A., Mazza A., Pressure drop in pipe lines for compressed air: comparison between experimental and theoretical analysis, transactions on Engineering Sciences vol 18, 1998, WIT Press, ISSN 1743-3533.